Understanding Emergent Dynamics through Modeling, Learning and Analysis

Baoli Hao

Research Advisors: Chun Liu, Ming Zhong

Illinois Institute of Technology

November 25, 2025

Introduction

Motivation: Complex Dynamics

(a) Fish Milling

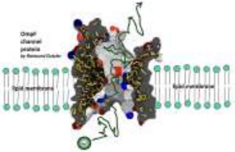

(b) Ion Transport

(c) Urban Crime

Figure: Complex dynamics arise from local interactions

Motivation

- *What mechanisms generate complex behavior?*
- *How can we infer the underlying interaction laws from observations?*
- *How can we provide theoretical guarantees for the resulting models?*

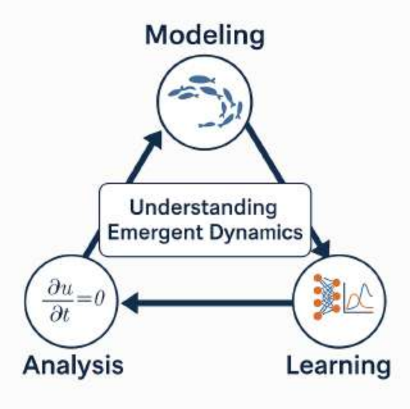

Outline

Part I – Modeling

Explain how local interactions create global patterns

Synchronization and Swarming

Patterns from phase–space coupling

Swarmalator Model [1]

How simple " phase + spatial" interactions generate surprising states?

$$\begin{aligned} \dot{x}_i &= \nu + \frac{J_i}{N} \sum_j^N \sin(x_j - x_i) \cos(\theta_j - \theta_i), \\ \dot{\theta}_i &= \omega + \frac{K_i}{N} \sum_j^N \sin(\theta_j - \theta_i) \cos(x_j - x_i), \quad (x_i, \theta_i) \in (\mathbb{S}^1, \mathbb{S}^1). \end{aligned} \tag{1}$$

- Real systems couple **motion** and **phase dynamics** (cells, robots, etc.).
- x_i-eq: attraction–repulsion forces (spatial swarming);
  θ_i-eq: Kuramoto phase coupling (phase synchronization).
- (ν, ω): constant natural frequencies; (J_i, K_i): couplings constants.
- Simple pairwise rules: interaction strength depends on **phase/spatial similarity**.
- **Minimal model** for exploring phase–spatial coupling and new emergent behaviors.
- **Energy:** $E = -\frac{A}{2N} \sum_{i,j} \cos(x_j - x_i) \cos(\theta_j - \theta_i)$, when $\nu = \omega = 0$, $J = K = A$.
  - gradient flow: $\dot{x}_i = -\frac{\partial E}{\partial x_i}$, $\dot{\theta}_i = -\frac{\partial E}{\partial \theta_i}$.

[1] O'Keeffe et al., 2017, *Nature communications.*

Positive-attractive and Negative-repulsive Couplings

- Set $J = 1$ and draw the phase coupling K from
  1. $h(K) = p\delta(K - K_p) + q\delta(K - K_n)$, where $p + q = 1$, $K_p > 0$ and $K_n < 0$
  2. Single Gaussian Distribution: $h(K) \sim \mathcal{N}(\mu, \sigma|K)$
  3. Mixed Gaussian Distribution: $h(K) \sim p\mathcal{N}(K_n, \sigma|K) + (1-p)\mathcal{N}(K_p, \sigma|K)$
- **Linear Stability Analysis:** compute the Jacobian matrix to determine local stability via eigenvalue analysis.
- **Numerical Simulation:** $W_\pm = S_\pm e^{-i\phi_\pm} := \frac{1}{N}\sum_{j=1}^{N} e^{i(x_j \pm \theta_j)}$ and $V := \frac{1}{N}\sum_{j=1}^{N}\langle|\dot{x}_j|\rangle_t$.

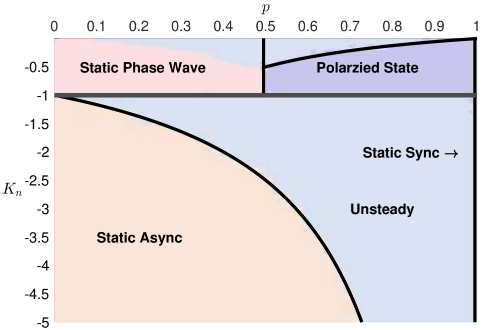

Phase Diagram on (p, K_n), $J = 1, K_p = 0.5$.

Behavior and Pattern [2]

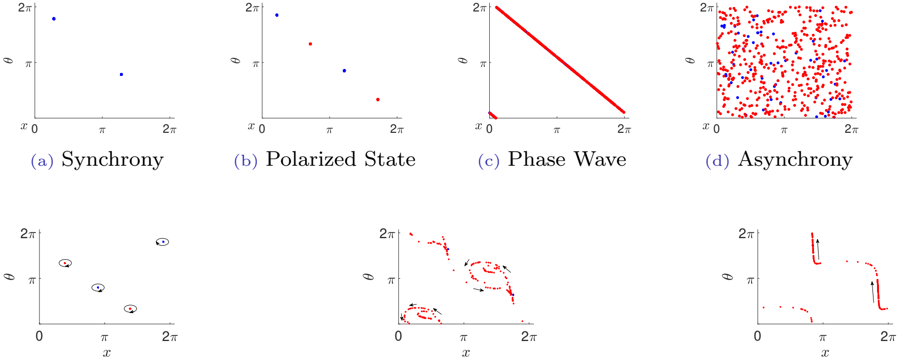

(a) Synchrony (b) Polarized State (c) Phase Wave (d) Asynchrony

(e) Breathing (f) Swirling (g) Active Bands

Figure: Top row: Steady States. Bottom Row: Unsteady States. Swarmalators coupling with K_p and K_n are presented as blue dots and red dots, respectively.

[2] Hao et al., 2023, *Physical Review E.*

Urban Crime Simulation

From agent rules to city-scale hotspot patterns

Motivation & Contributions

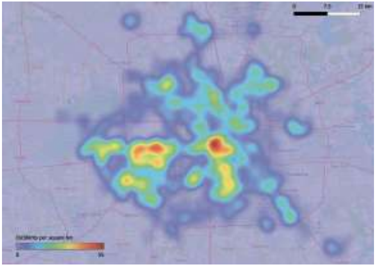

How local criminal decision-making and environmental factors generate city-scale crime patterns?

Goal

Build a **realistic, efficient, FEM framework** for burglary dynamics.

Why agent-based model?

- Offender movement and burglary decisions are **probabilistic**
- ABM capture individual behavior

Why PDE?

- Too many agents $\Rightarrow$ expensive, noisy
- Hard to predict long-term patterns
- Large populations $\Rightarrow$ **mean-field limit**: describing **aggregation**
- PDE reveals macroscopic mechanisms of hotspot formation

Why Natural BCs & FEM?

- Offenders do not "wrap around" the domain
- Realistic city shapes, heterogeneous parameters
- Natural BCs enforced naturally

Models [3]

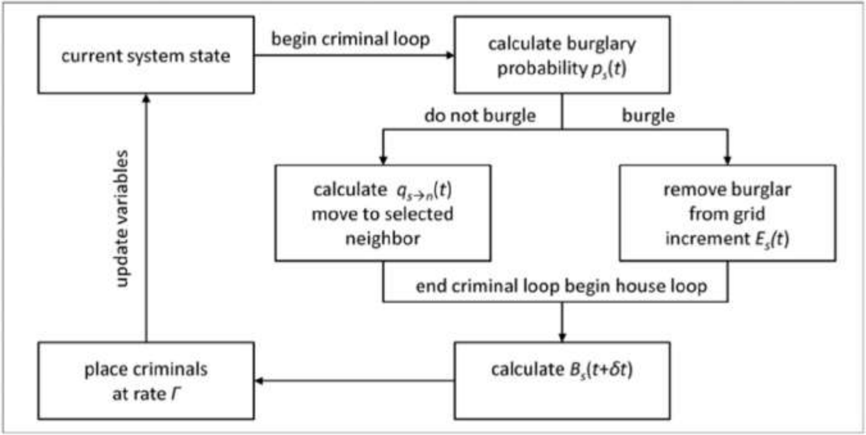

[3] Short et al., 2008, *Mathematical Models and Methods in Applied Sciences.*

Models

- Agent-based Model:

$$B_s(t+\Delta t) = \left[(1-\eta)B_s(t) + \frac{\eta}{4}\sum_{s'\sim s} B_{s'}(t)\right](1-\omega\Delta t) + \theta E_s(t)$$

$$n_s(t+\Delta t) = A_s \sum_{s'\sim s} \frac{n_{s'}(t)[1-p_{s'}(t)]}{T_{s'}(t)} + \Gamma\Delta t, \quad T_{s'}(t) = \sum_{s''\sim s'} A_{s''}(t).$$

- B_s: attractiveness at site s; n_s: number of criminals at site s; Γ: burglars generation rate; θ: increase in attractiveness due to one burglary event; ω: dynamic attractiveness decay rate; $E_s(t)$ is the number of burglary events that occurred at site s during the time interval beginning at time t; $p_s(t) = 1 - e^{-A_s(t)\Delta t}$: burglary probability.
- PDE Model (dimensionless mean-field limit):

$$\frac{\partial A}{\partial t} - \eta\Delta A + A - \rho A = -\eta\Delta A^{st} + A^{st}, \quad \frac{\partial \rho}{\partial t} - \nabla\cdot\left(\nabla\rho - \frac{2\nabla A}{A}\rho\right) + \rho A = \frac{\Gamma\theta}{\omega^2}.$$

- $A = B + A^{st}$; ρ: density of criminals.
- η: measures the significance of neighborhood effects; $\frac{\Gamma\theta}{\omega^2}$: influx of criminals.

FEM Framework and Patterns [4]

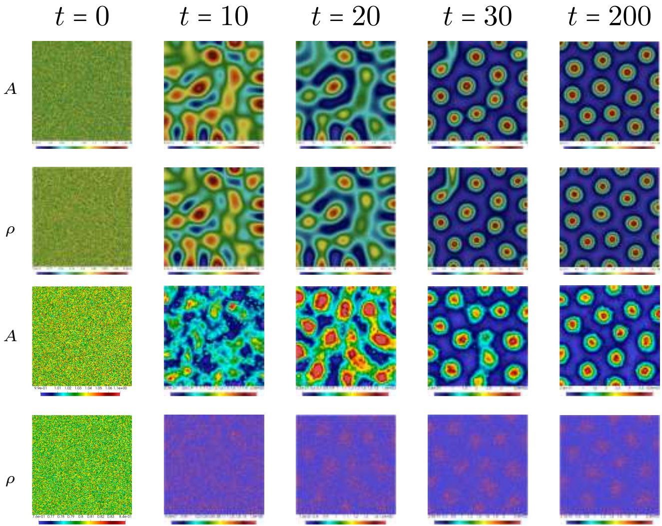

[4] Hao et al., 2025, *Mathematical Models and Methods in Applied Sciences.*

How parameters affect the pattern?

- $\eta \in [0, 1]$: measures the significance of neighborhood effects
- $\frac{\Gamma\theta}{\omega^2}$: influx of criminals

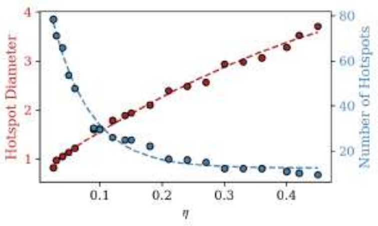

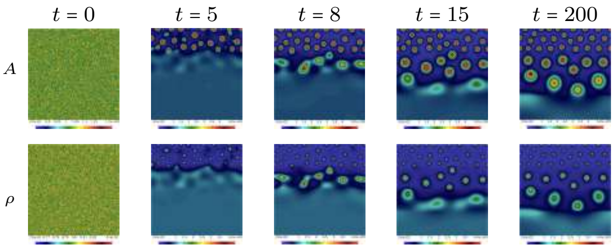

Robustness and Validation

$(h, \Delta t)$	Case 1			Case 2			Case 3		
	10^{-3}	10^{-6}	10^{-9}	10^{-3}	10^{-6}	10^{-9}	10^{-3}	10^{-6}	10^{-9}
$(\frac{16}{400}, \frac{1}{100})$	1.01	1.10	1.14	1.02	1.67	2.65	1.04	2.73	4.88
$(\frac{16}{200}, \frac{1}{50})$	1.01	1.11	1.26	1.04	1.89	2.96	1.08	3.06	5.93
$(\frac{16}{100}, \frac{1}{25})$	1.02	1.13	1.31	1.07	2.11	3.39	1.17	3.16	6.04
$(\frac{16}{100}, \frac{2}{25})$	1.03	1.15	1.38	1.11	2.34	4.17	-	-	-

Table: Average number of iterations over time required by the iterative splitting algorithm to meet the stopping crieterion with $\texttt{tol}_1 = \texttt{tol}_2 = 10^{-3}, 10^{-6}, 10^{-9}$ for the three cases with different values of mesh size h and time step Δt.

Spatial Heterogeneity & Complex Geometry

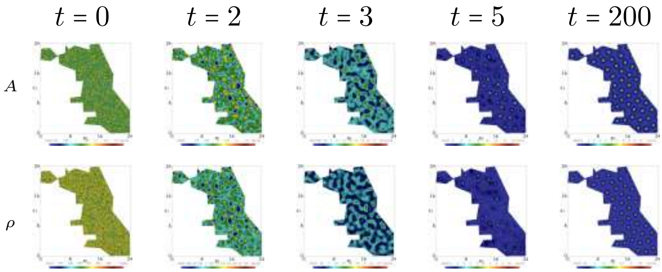

Figure: Chicago Simulation

Highway I-90 Animation:

$$A^{st}(\boldsymbol{x}) = \frac{1}{30} \cdot \exp\{-20 * (x_0 + x_1 - l)^2\} \cdot \left(x_0 > \frac{l}{2} \ \& \ x_1 < \frac{l}{2}\right) + \frac{1}{30} \cdot \chi_1(\boldsymbol{x}),$$

$$\frac{\Gamma(\boldsymbol{x})\theta}{\omega^2} = B_0(\boldsymbol{x}) = \exp\{-20 * (x_0 + x_1 - l)^2\} \cdot \left(x_0 > \frac{l}{2} \ \& \ x_1 < \frac{l}{2}\right) + 1 \cdot \chi_{0.1}(\boldsymbol{x}).$$

https://github.com/baolihao/UrbanCrime-Sim

Part II – Learning

Learn the hidden rules and dynamical laws from data

Learning Kernels

Recovering interaction laws from steady states

Motivation

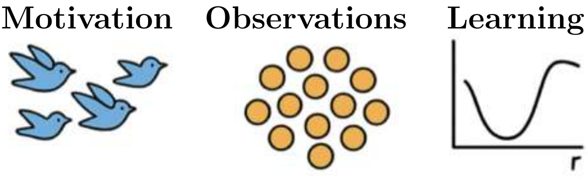

- Many complex systems (flocking, swarming, opinion dynamics) evolve according to **unknown interaction laws**.
- Existing methods require **time-series data**, **large samples**, or assume simple parametric forms [5].
- **Limited data:** We have only **steady-state snapshots** rather than full trajectories.
- **Highly underdetermined**: forces cancel out, time-scale disappears, and the system becomes **ill-conditioned**.
- Goal: develop a **robust, data-efficient framework** that can recover interaction laws **from a single steady-state snapshot**.

[5] Lu et al., 2019, *Proceedings of the National Academy of Sciences.*

Problem Setup

- The first-order dynamics:

$$\dot{\mathbf{x}}_i = \sum_{j \neq i}^{N} \frac{1}{N} \phi^E(|\mathbf{x}_j - \mathbf{x}_i|)(\mathbf{x}_j - \mathbf{x}_i). \tag{2}$$

- The second-order dynamics:

$$\begin{cases} \dot{\mathbf{x}}_i &= \mathbf{v}_i, \\ \dot{\mathbf{v}}_i &= \sum_{j \neq i}^{N} \frac{1}{N}\Big(\phi^E(|\mathbf{x}_j - \mathbf{x}_i|)(\mathbf{x}_j - \mathbf{x}_i) + \phi^A(|\mathbf{x}_j - \mathbf{x}_i|)(\mathbf{v}_j - \mathbf{v}_i)\Big). \end{cases} \tag{3}$$

- Given: A set of single-time snapshots at steady state $\{\mathbf{x}_{i,T_m}^m\}_{i,m=1}^{N,M}$ or $\{\mathbf{x}_{i,T_m}^m, \mathbf{v}_{i,T_m}^m\}_{i,m=1}^{N,M}$.
- Goal: Learn ϕ^E or ϕ^A to get approximated $\hat{\phi}^E$ or $(\hat{\phi}^E, \hat{\phi}^A)$.

Learning Framework

Nonlinear Interaction Dynamics

$$0 = \sum_{j \neq i} \phi(r_{ij})\, \mathbf{r}_{ij}$$

$\Downarrow$

Finite-Dimensional Representation of Kernel

$$\phi(r) \approx \sum_k \alpha_k\, \psi_k(r)$$

$\Downarrow$

Linear System at Steady State

$F(\alpha; \mathbf{x}) = A(\mathbf{x})\alpha = 0$, F: a **rank-deficient linear operator**

$\Downarrow$

Nullspace / Eigenstructure Extraction

Ill-conditioning: $F(C\alpha; \mathbf{x}) = F(\alpha; \mathbf{x}) = 0, \forall C \in \mathbb{R}$

$\Downarrow$

Scaling Recovery (Time-Scaling or Energy)

Determine physical scale C of $\hat{\phi}$: $\phi \sim C\hat{\phi}$

Ill-conditioning & Regularization

At steady state:

$$\sum_{j\neq i} \phi(|\mathbf{x}_j - \mathbf{x}_i|)(\mathbf{x}_j - \mathbf{x}_i) = 0.$$

Ill-conditioning: Steady-state equations do not contain enough information to uniquely determine ϕ without **additional constraints or scaling information**.

- **Empirical Distribution Regularization (and Learnability Check):**

  $$\rho_T(r) = \mathbb{E}\left[\delta_{r_{i,j,T}}(r)\right], \quad r_{i,j,T} = |\mathbf{x}_{j,T} - \mathbf{x}_{i,T}|.$$

  $\longrightarrow$ ρ_T is not learnable when the geometry of the steady-state distribution does not produce enough linear constraints on ϕ (Identifiability requires $\dim\ker F \le 1$).
- **Minimal Energy Direction (Crucial Missing Information):**
  For gradient-flow dynamics, true steady states are **energy minimizers**:
  $E = \frac{1}{N}\sum_{i<j} U(|\mathbf{x}_j - \mathbf{x}_i|), \quad U'(r) = r\,\phi(r).$
  This provides the **missing information (but available)** to select the correct ϕ.
  $\longrightarrow$ Combined with $\nabla E = 0$, if the learned ϕ increases E, flip its sign: $\phi \leftarrow -\phi$.
- **Time-scale Recovery:**
  If one trajectory or a steady-state time T_m is known, estimate scaling C by minimizing

  $$\|T_m - \hat{T}_m(C)\|.$$

Results: Adaptive Learning

- The use of nonuniform knots allows to focus more on regions of the domain where data points are densely concentrated, while reducing resolution in regions with sparse data.

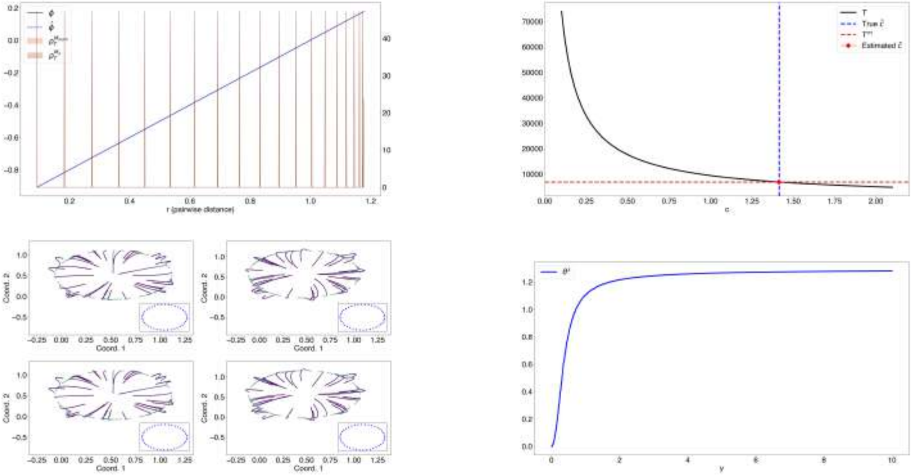

Figure: Kernel: $r - 1$

Results

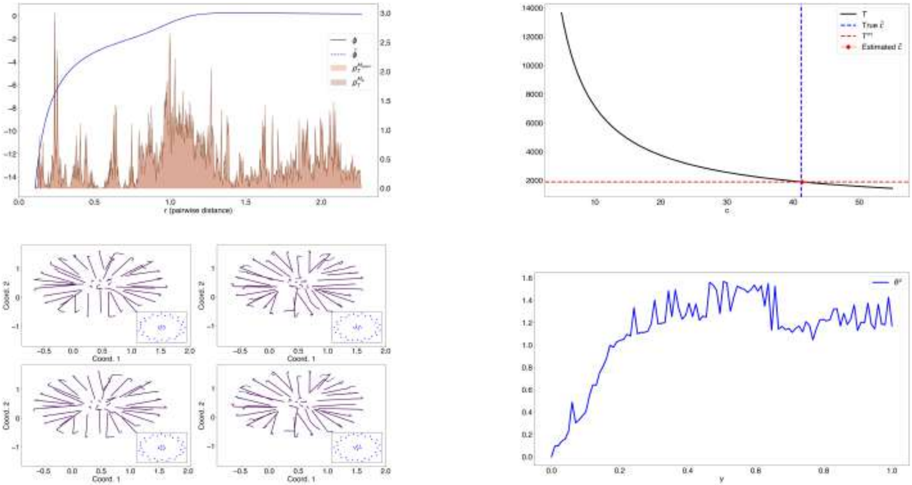

Figure: Kernel: tanh

Results

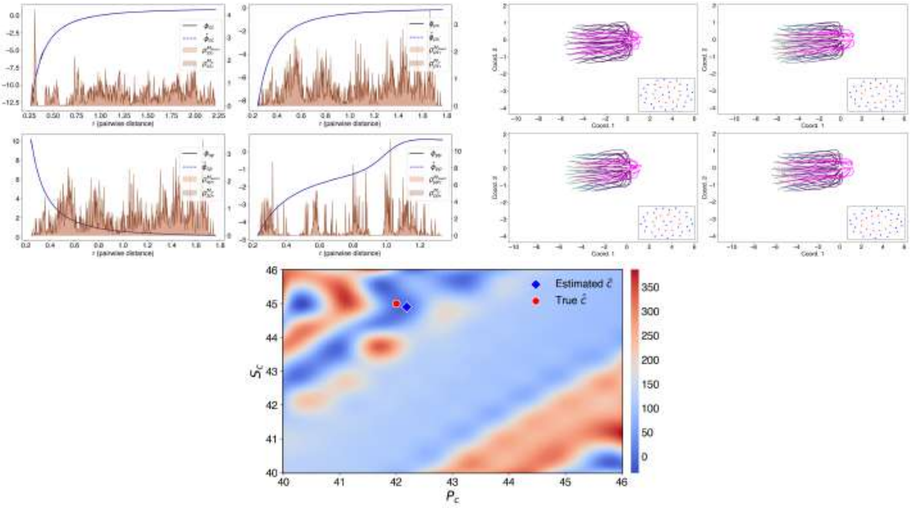

Figure: Kernel: Multi-species

Results

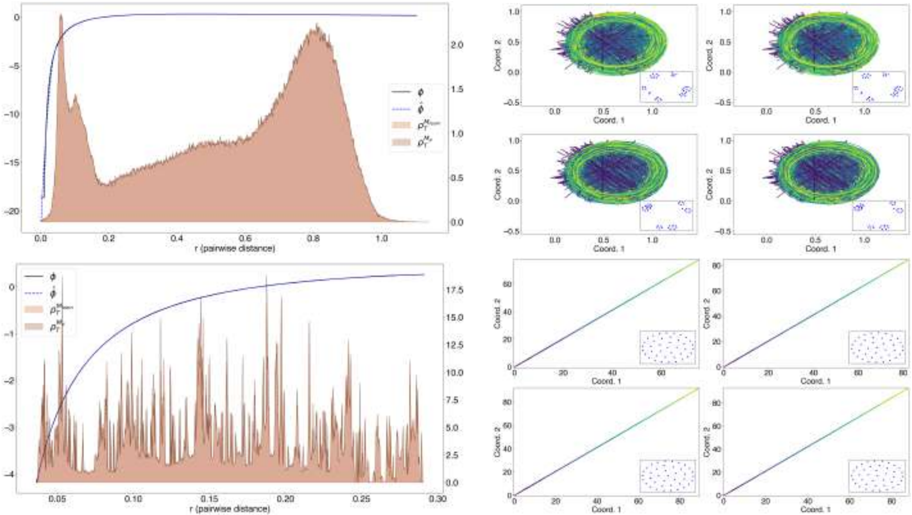

Figure: Kernel: Fish Milling & Flocking

Part III – Analysis

Provide mathematical foundations for well-posedness

Stability in Training PINNs

Stability in Training PINNs for Stiff PDEs: Why Initial Conditions Matter

Introduction to PINNs [6,7]

- PINNs integrate PDE constraints into deep learning

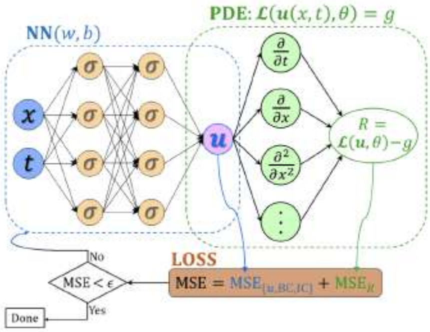

Figure: Schematic of PINN, where the loss function of PINN contains a mismatch in the given data on the state variables or boundary and initial conditions. The hyperparameters of PINN can be learned by minimizing the total loss $\mathcal{L} = MSE_{IC} + MSE_{BC} + MSE_R$.

[6] Lagaris et al., 1998, *IEEE transactions on neural networks.*

[7] Raissi et al., 2019, *Journal of Computational physics.*

Motivation & Contributions

Why enforcement of IC matters?

- Training PINNs on **stiff PDEs** is highly unstable.
- Stiff PDEs evolve on **widely varying time scales**.
- Explicit solvers struggle $\longrightarrow$ stability hinges on **ICs**.
- Soft penalty causes severe **spectral bias**, and failure to propagate information away from $t = 0$.

Main Contributions:

- Systematic **ablation study** of stabilization mechanisms for stiff PDEs.
- Show hard IC constraints are the dominance for stability and accuracy.
- Demonstrate effectiveness across **7 stiff PDE benchmarks** (AC, CH, GS, KS, LA, etc.).
- Provide an **NTK-based theoretical explanation** for why hard IC constraints reduce spectral bias and improve training decay rates.
- Show compatibility with advanced PINN techniques (causal PINNs, RBA PINNs, time-marching, etc.).

Methodology

- PDE setup: $u_t + \mathcal{P}(u) = f$ on $(0,T] \times \Omega$.
- **Hard constraint transformation:**

$$\tilde{u}(t,\boldsymbol{x}) = \psi(t,\boldsymbol{x}) + \phi(t,\boldsymbol{x}) u_{\mathrm{NN}}(t,\boldsymbol{x}),$$

  with $\psi(0,\boldsymbol{x}) = u_0(\boldsymbol{x}), \phi(0,\boldsymbol{x}) = 0$ ensuring exact IC satisfaction.
- Standard PINN loss combines:

$$\mathcal{L} = \mathcal{L}_{\mathrm{IC/BC}} + \mathcal{L}_{\mathrm{R}}.$$

- HC-PINN loss:

$$\mathcal{L} = \mathcal{L}_{\mathrm{R}}.$$

Summary

- Hard ICs enforce the time direction in training, reducing spectral bias **(NTK)**.
- Mimics traditional numerical solvers (exact ICs at $t = 0$).
- Behaves like an implicit time integrator $\rightarrow$ more stable.

Results

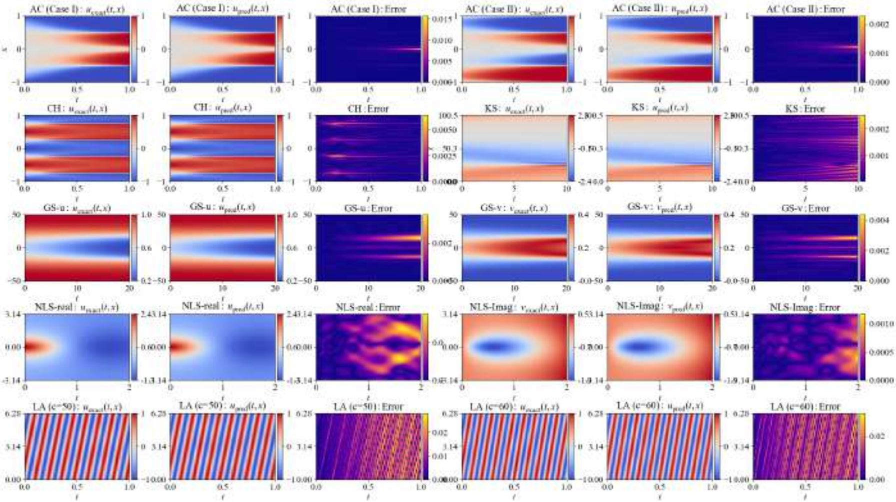

Figure: Benchmark Results: Truth vs HC-PINN vs Absolute Error.

Results: Comparison

	Causal training (MLP)[8]	Enhanced RBA[9]	HC-PINNs
AC (Case I)	6.95×10^{-2}	2.62×10^{-3}	8.29×10^{-4}
AC (Case II)	1.78×10^{-2}	1.08×10^{-3}	2.14×10^{-4}
CH	3.49×10^{-1}	9.83×10^{-2}	5.61×10^{-4}
KS	2.72×10^{-1}	3.64×10^{-2}	5.37×10^{-4}

Table: Relative L^2 errors after $50k$ training iterations. All methods are implemented under the same $50k$ iteration.

- HC-PINNs achieve much lower errors with fewer iterations!

[8] Wang et al., 2022, *arXiv preprint arXiv:2203.07404.*

[9] Anagnostopoulos et al., 2023, *arXiv preprint arXiv:2307.00379.*

Ion transport: PNP

Rigorous analysis for complex ion transport PDEs

Variational Models [10]

- Variational models are useful in modeling problems in physics, biology, etc.
- Variational models leverages the laws of thermodynamics to model chemo-mechanical effects across different scales in a unified way:
  - 1st law of thermodynamics: $\frac{d}{dt}(\mathcal{K}+\mathcal{U}) = \dot{\mathcal{W}} + \dot{\mathcal{Q}}$.
  - 2nd law of thermodynamics: $Td\mathcal{S} = \dot{\mathcal{Q}} + \triangle$ with $\triangle \geq 0$.

  $\mathcal{K}$: kinetic energy; $\mathcal{F}$: free energy; $\dot{\mathcal{W}} = 0$: rate of external work; $\dot{\mathcal{Q}}$: rate of heat absorbed; $\triangle \geq 0$: rate of entropy production.

Energy-dissipation law (Isothermal Case)

$$\frac{d}{dt}E^{total} = \frac{d}{dt}(\mathcal{K}+\mathcal{F}) = \dot{\mathcal{W}} - \triangle,$$

where $\mathcal{F} := \mathcal{U} - T\mathcal{S}$.

- Capable to incorporate multiscale chemo-mechanical coupling systematically by choosing appropriate energy and the rate of energy-dissipation.
- Force (mechanical) and reaction rate (chemical) can be derived using **EnVarA**.

[10] Giga et al., 2018, *Handbook of mathematical analysis in mechanics of viscous fluids.*

Introduction to PNP Equations [11]

- **Ion transport is fundamental:** Appears in electrochemistry, physiology (ion channels), semiconductors, energy storage, porous media.
- **Microscopic description is too complex:** Direct particle-based models are computationally expensive.

Poisson-Nernst-Planck (PNP) Equations:

$$\partial_t c_i = -\nabla \cdot \boldsymbol{J}_i, \qquad \boldsymbol{J}_i = -D_i \nabla c_i - \frac{D_i z_i e}{k_B T} c_i \nabla \phi,$$
$$-\nabla \cdot (\epsilon \nabla \phi) = \sum_i z_i e c_i, \qquad \text{where} \quad i = n, p.$$

Energy and Dissipation:

$$E[c_n, c_p, \phi] = \int_\Omega k_B T (c_n \ln \frac{c_n}{c_{n\infty}} + c_p \ln \frac{c_p}{c_{p\infty}}) + \frac{\epsilon}{2} |\nabla \phi|^2 \, dx.$$
$$\triangle = \int_\Omega \frac{k_B T}{D_n} c_n |\boldsymbol{u}_n|^2 + \frac{k_B T}{D_p} c_p |\boldsymbol{u}_p|^2 \, dx.$$

[11] Xu et al., 2014, *Communications in Mathematical Physics.*

PNP with Steric Effects [12] and Relative Drags

- **Classical PNP is a dilute-solution mean–field model.**
- **High ionic concentration / crowding [13]:** Finite size and excluded-volume effects lead to nonlinear correlations. Strong ion–ion and ion–solvent interactions require including steric repulsion, cross interactions.
- **Coupled friction and relative drags [14]:** In crowded electrolytes, ions do not move independently. When a cation moves, it drags nearby anions (cross diffusion).
- **Modification:**

$$\mathcal{A}^* = \int_\Omega k_B T \left(c_n \ln \frac{c_n}{c_{n\infty}} + c_p \ln \frac{c_p}{c_{p\infty}} + \frac{1}{2} g_{nn} c_n^2 + g_{np} c_n c_p + \frac{1}{2} g_{pp} c_p^2 \right) + \frac{\epsilon}{2} |\nabla \phi|^2 \, dx,$$

$$\triangle^* = \int_\Omega \frac{k_B T}{D_n} c_n |\boldsymbol{u}_n^*|^2 + \frac{k_B T}{D_p} c_p |\boldsymbol{u}_p^*|^2 + \frac{K_B T}{D_{n,p}} c_n c_p |\boldsymbol{u}_n^* - \boldsymbol{u}_p^*|^2 \, dx,$$

where $g_{nn}, g_{pp} > 0$: self-crowding repulsion and g_{np}: cross-crowding effect between cations and anions, $D_{n,p}$ is a cross-diffusion or friction coefficient.

[12] Horng et al., 2012, *The Journal of Physical Chemistry B.*

[13] Hsieh, 2019, *Nonlinear Analysis: Real World Applications.*

[14] Hsieh et al., 2015, *Journal of Mathematical Analysis and Applications.*

PNP with Steric Effects and Relative Drags

$$
\begin{aligned}
\partial_t c_n =& \nabla \cdot \Big[\frac{D(1+c_n)}{1+c_n+c_p} \Big(\nabla c_n + \frac{z_n e}{k_B T} c_n \nabla \phi + \frac{g_{nn}}{k_B T} c_n \nabla c_n + \frac{g_{np}}{k_B T} c_n \nabla c_p \Big) \\
&+ \frac{D c_n}{1+c_n+c_p} \Big(\nabla c_p + \frac{z_p e}{k_B T} c_p \nabla \phi + \frac{g_{pp}}{k_B T} c_p \nabla c_p + \frac{g_{np}}{k_B T} c_p \nabla c_n \Big) \Big], \\
\partial_t c_p =& \nabla \cdot \Big[\frac{D(1+c_p)}{1+c_n+c_p} \Big(\nabla c_p + \frac{z_p e}{k_B T} c_p \nabla \phi + \frac{g_{pp}}{k_B T} c_p \nabla c_p + \frac{g_{np}}{k_B T} c_p \nabla c_n \Big) \\
&+ \frac{D c_p}{1+c_n+c_p} \Big(\nabla c_n + \frac{z_n e}{k_B T} c_n \nabla \phi + \frac{g_{nn}}{k_B T} c_n \nabla c_n + \frac{g_{np}}{k_B T} c_n \nabla c_p \Big) \Big], \\
-\epsilon \Delta \phi =& z_p c_p + z_e c_n.
\end{aligned}
$$

- Produces diffusion matrices, can lose symmetry or positivity.
- Becomes degenerate, non-symmetric, and no longer variational.

PNP with Steric Effects and Relative Drags

To simplify the equations, we let $u = c_n + c_p, \quad v = c_n - c_p$.

$$\begin{aligned}\partial_t u =&\nabla\cdot\big[\nabla u - v\nabla\phi + u\nabla u\big],\\ \partial_t v =&\nabla\cdot\Big[\frac{1}{1+u}(\nabla v - u\nabla\phi + v\nabla u) + \frac{v}{1+u}(\nabla u - v\nabla\phi + u\nabla u)\Big],\\ \Delta\phi =&v,\end{aligned} \tag{4}$$

with boundary conditions:

$$\begin{aligned}(\nabla v - u\nabla\phi + v\nabla u)\cdot\nu &= 0,\\ (\nabla u - v\nabla\phi + u\nabla u)\cdot\nu &= 0,\\ \phi &= 0,\end{aligned}$$

and initial conditions:

$$\begin{aligned}u(x,0) = u^0(x) = c_n^0(x) + c_p^0(x) \in L^2(\Omega),\\ v(x,0) = v^0(x) = c_n^0(x) - c_p^0(x) \in L^2(\Omega).\end{aligned}$$

Main Theorem and A Priori Estimate

Lemma 1

Let (u,v) be the solution. Then there exist positive constants K_1, K_2 and γ depending only on M_0, d, and Ω such that

$$\frac{d}{dt}\Big(\int_\Omega K_1 u^2 + v^2\,dx\Big) + \gamma\int_\Omega \big(|\nabla u|^2 + |\nabla v|^2\big)\,dx + K_1\int_\Omega \bar{u}^*|\nabla u|^2\,dx$$
$$\le K_2\big(1 + \|\bar{v}\|^4_{L^2(\Omega)}\big)\Big(\int_\Omega K_1 u^2 + v^2\,dx\Big).$$

Main Theorem (Local Existence)

Suppose that the initial data $c_{n,0}, c_{p,0} \in L^\infty(\Omega)$. Then there exists $t_0 > 0$ such that the PDE system 4 has a solution (c_n, c_p, ϕ) with
$0 \le c_n, c_p \in L^\infty((0,t_0); L^2(\Omega)) \cap L^2((0,t_0); H_1(\Omega))$ and
$\partial_t c_n, \partial_t c_p \in L^2((0,t_0); H^{-1}(\Omega))$.

Proof Outlines

Fixed Point Framework:

- Define $F((\bar{u},\bar{v})) = (u,v)$ in $X = \{(f,g) : f,g \in L^4((0,t_1);L^2(\Omega))\}$.
- Truncation: $f^* = \min\{\max(f,0), 5M_0\}$
- The elliptic equation $\Delta\bar{\phi} = \bar{v}$ couples the system.

Galerkin Approximation and Compactness:

- Apply Galerkin's method to construct approximate (u^k, v^k).
- Use the a priori estimate and Gronwall's inequality for uniform bounds:

$$(u^k, v^k) \text{ bounded in } L_t^\infty L_x^2 \cap L_t^2 H_x^1.$$

- Compactness $\Rightarrow$ continuity of F and $F(B_R) \subset B_R$.

Passing to the Limit:

- Apply Schauder's fixed point theorem to obtain a fixed point (u,v).
- Recover (c_n, c_p) and ϕ, proving local existence and positivity.

Results

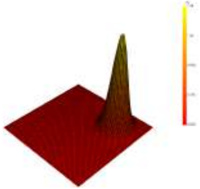

(a) c_n: Time Step = 0

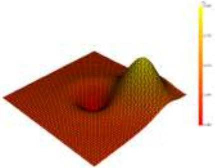

(b) c_n: Time Step = 30

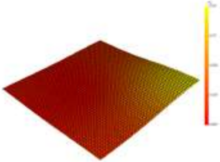

(c) c_n: Time Step = 380

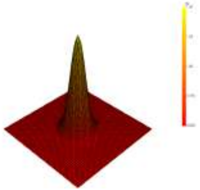

(d) c_p: Time Step = 0

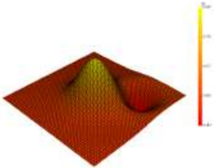

(e) c_p: Time Step = 30

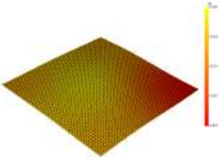

(f) c_p: Time Step = 380

Results

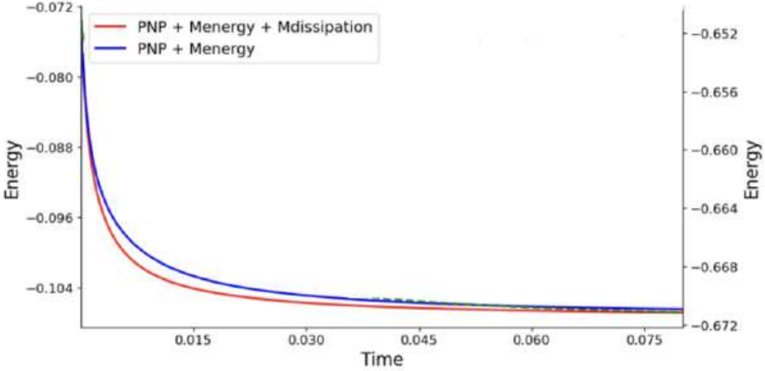

Figure: Comparison between different models

Synthesis and Outlook

Conclusion

- Emergent behavior across physical, biological, and social systems can be explained by **interaction rules**.
  $\longrightarrow$ Examples: Swarmalators; Crime models; Ion transport systems
- If emergent patterns reflect interaction rules, we can **recover** the rules from the patterns.
  $\longrightarrow$ Examples: Learning kernels from steady states
- Predictive models require **mathematical foundations**: existence, stability, and structure.
  $\longrightarrow$ Examples: Global existence for nonlinear PDEs; Stability in training PINNs

Ongoing and Future Work

1. **Synchronization and Swarming:** Extending this work to networked graph systems.
2. **Crime Pattern Modeling:** Extending the model to include police response for data-driven predictive analytics and decision support in complex systems.
3. **Learning Kernels:** Developing a topological learning framework that leverages persistent homology to infer interaction laws from spatial patterns by integrating neighborhood density information with geometric and dynamical features of the data.
4. **PINNs:** Combining Physics-Informed Neural Networks with Graph Neural Networks to model biological interactions.
5. **Ion transport and PNP:** Ongoing work focuses on establishing the global existence of weak solutions near equilibrium.

References I

[1] Sokratis J Anagnostopoulos, Juan Diego Toscano, Nikolaos Stergiopulos, and George Em Karniadakis. Residual-based attention and connection to information bottleneck theory in pinns. *arXiv preprint arXiv:2307.00379*, 2023.

[2] Mi-Ho Giga, Arkadz Kirshtein, and Chun Liu. Variational modeling and complex fluids. In *Handbook of mathematical analysis in mechanics of viscous fluids*, pages 73–113. Springer, 2018.

[3] Baoli Hao, Ming Zhong, and Kevin O'Keeffe. Attractive and repulsive interactions in the one-dimensional swarmalator model. *Physical Review E*, 108(6):064214, 2023.

[4] Baoli Hao, Kamrun Mily, Annalisa Quaini, and Ming Zhong. A finite element framework for simulating residential burglary in realistic urban geometries. *arXiv preprint arXiv:2508.11055*, 2025.

[5] Tzyy-Leng Horng, Tai-Chia Lin, Chun Liu, and Bob Eisenberg. Pnp equations with steric effects: a model of ion flow through channels. *The Journal of Physical Chemistry B*, 116(37):11422–11441, 2012.

[6] Chia-Yu Hsieh. Global existence of solutions for the poisson–nernst–planck system with steric effects. *Nonlinear Analysis: Real World Applications*, 50:34–54, 2019.

[7] Chia-Yu Hsieh, YunKyong Hyon, Hijin Lee, Tai-Chia Lin, and Chun Liu. Transport of charged particles: entropy production and maximum dissipation principle. *Journal of Mathematical Analysis and Applications*, 422(1):309–336, 2015.

References II

[8] Isaac E Lagaris, Aristidis Likas, and Dimitrios I Fotiadis. Artificial neural networks for solving ordinary and partial differential equations. *IEEE transactions on neural networks*, 9(5):987–1000, 1998.

[9] Fei Lu, Ming Zhong, Sui Tang, and Mauro Maggioni. Nonparametric inference of interaction laws in systems of agents from trajectory data. *Proceedings of the National Academy of Sciences*, 116(29):14424–14433, 2019.

[10] Kevin P O'Keeffe, Hyunsuk Hong, and Steven H Strogatz. Oscillators that sync and swarm. *Nature communications*, 8(1):1504, 2017.

[11] Maziar Raissi, Paris Perdikaris, and George E Karniadakis. Physics-informed neural networks: A deep learning framework for solving forward and inverse problems involving nonlinear partial differential equations. *Journal of Computational physics*, 378:686–707, 2019.

[12] Martin B Short, Maria R D'orsogna, Virginia B Pasour, George E Tita, Paul J Brantingham, Andrea L Bertozzi, and Lincoln B Chayes. A statistical model of criminal behavior. *Mathematical Models and Methods in Applied Sciences*, 18(supp01): 1249–1267, 2008.

[13] Sifan Wang, Shyam Sankaran, and Paris Perdikaris. Respecting causality is all you need for training physics-informed neural networks. *arXiv preprint arXiv:2203.07404*, 2022.

[14] Shixin Xu, Ping Sheng, and Chun Liu. An energetic variational approach for ion transport. *arXiv preprint arXiv:1408.4114*, 2014.

Thank you ! Happy Thanks Giving !